

# Analysis of size effect on strength of quasi-brittle materials using integral-type nonlocal models



Petr Havlásek<sup>a</sup>, Peter Grassl<sup>b,\*</sup>, Milan Jirásek<sup>a</sup>

<sup>a</sup> Department of Mechanics, Faculty of Civil Engineering, Czech Technical University in Prague, Czech Republic

<sup>b</sup> School of Engineering, University of Glasgow, Glasgow, UK

## ARTICLE INFO

### Article history:

Received 21 May 2015

Received in revised form 22 December 2015

Accepted 17 February 2016

Available online 23 February 2016

### Keywords:

Nonlocal model

Damage mechanics

Fracture

Calibration

Size effect

Concrete

Boundaries

## ABSTRACT

The influence of the averaging operator of nonlocal continuum damage models near specimen boundaries on the size effect on strength of quasibrittle materials is investigated. Two phenomenological approaches, namely standard rescaling and distance-based models, are considered. The numerical results are compared to data from three-point bending tests of notched and unnotched beams recently reported in the literature. It is shown that both approaches can reproduce the experiments well for one type of geometry with one set of input parameters. However, only the distance-based model provides a good agreement for both unnotched and notched beams with the same set of parameters.

© 2016 The Authors. Published by Elsevier Ltd. This is an open access article under the CC BY license (<http://creativecommons.org/licenses/by/4.0/>).

## 1. Introduction

The fracture process in quasi-brittle heterogeneous materials is characterised by a softening response in the form of decreasing force with increasing displacement. Structures made of such materials exhibit a strong size effect: small structures possess a greater nominal strength than large ones. For structures of practical size, this size effect follows neither the plastic limit load theory nor linear elastic fracture mechanics. Furthermore, it strongly depends on the type of boundaries of structures. For instance, notched and unnotched structures exhibit different types of size effects, which was recently demonstrated by two independent sets of experiments reported in Grégoire et al. [11] and Hoover et al. [12]. The special feature of these two studies in comparison to other existing experimental work is that the specimens with different boundaries are all made of the same batch of concrete and tested under the same conditions. Therefore, they form a suitable reference for evaluating the performance of constitutive models for concrete fracture.

Modelling of the fracture process in quasibrittle materials is challenging since the fracture process zone, defined as the zone in which energy is dissipated, is influenced by the heterogeneities of the material, and possesses a finite width. A phenomenological description of the width of the fracture process zone can be obtained by enhanced constitutive models equipped by an internal material length, e.g., by integral-type nonlocal models, which link the softening process to weighted spatial averages of history variables [23,15]. Commonly, the weighted averaging is performed isotropically with the radius of the support of the weight function as an additional material parameter. These integral-type nonlocal models are often used

\* Corresponding author. Tel.: +44 141 330 5208.

E-mail address: [peter.grassl@glasgow.ac.uk](mailto:peter.grassl@glasgow.ac.uk) (P. Grassl).

## Nomenclature

$b$	out-of-plane thickness
$D$	depth of the beam
$d$	minimum distance to the boundary
$\mathbf{D}_e$	isotropic elastic stiffness tensor
$E$	Young's modulus
$F$	loading force
$L$	beam span
$R$	parameter reflecting the internal length
$t$	time
$V$	integration domain
$\alpha$	weight function
$\alpha_0, \gamma$	auxiliary functions in the weight function $\alpha$
$\beta, \eta$	dimensionless parameters in the weight function $\alpha$
$\boldsymbol{\varepsilon}$	strain
$\varepsilon_{eq}$	local equivalent strain
$\bar{\varepsilon}_{eq}$	nonlocal equivalent strain
$\varepsilon_0, \varepsilon_f$	dimensionless parameters in the damage function
$\kappa_d$	history variable in damage model
$\lambda$	relative notch depth
$\nu$	Poisson's ratio
$\boldsymbol{\sigma}$	stress
$\bar{\boldsymbol{\sigma}}$	effective stress
$\sigma_n$	nominal stress
$\omega$	damage variable

for finite element analyses of fracture processes, since they reproduce fracture patterns independently of the mesh, for both localised and distributed cracking, and are insensitive to the finite element mesh alignment. Therefore, they are considered to be more versatile than alternative models, such as crack band and cohesive crack approaches, which provide mesh-size independent results for localised cracking only, and are often sensitive to the alignment of the finite element mesh.

Nevertheless, the performance of nonlocal models still needs to be improved. Research topics that require attention include the calibration of the nonlocal characteristic length and the treatment of boundaries. The present work addresses the latter issue and can be seen as an application of the work in [10], in which the local energy dissipation of different nonlocal models close to nonconvex boundaries was investigated. Our objective is to investigate the impact of the specific form of the averaging operator on the prediction of size effect results. We are not aiming to demonstrate any potential superiority of nonlocal models over other techniques to model fracture.

Since the type of averaging is chosen phenomenologically, it is not clear how the averaging procedure should be influenced by specimen boundaries. One frequently used requirement is that, after the spatial averaging, uniform fields of history variables should remain uniform over the entire specimen. Therefore, the weighted average is usually rescaled by the integral of the weight function over the specimen domain included in the averaging. Models using only this approach to deal with boundaries shall be referred to as standard. More advanced techniques for treating boundaries have been proposed in the literature. For instance, the nonlocal weight function may depend on the distance to the boundaries [6,19,3,10], or on the stress state [1,14,8,10]. The performance of typical formulations of standard, distance-based and stress-based models has recently been compared to results of meso-scale analyses of fracture in beams with nonconvex boundaries by Grassl et al. [10].

Nonlocal models with standard averaging are the most commonly used. These models can be calibrated to fit the size effect exhibited by concrete for one type of boundary at a time [5,18]. However, it was reported in Grégoire et al. [11] that this type of model cannot be calibrated to give a good fit for the size effect on strength for specimens with different type of boundaries for one set of input parameters. This finding is surprising since other modelling techniques, such as cohesive crack [13] and meso-scale approaches [9,7], have been shown to be capable of predicting the size effect of notched and unnotched specimens with one set of parameters. This apparent shortcoming of the standard nonlocal models serves as motivation for the present study. The hypothesis is that the shortcoming originates from spurious strengthening of zones close to notches introduced by the phenomenological spatial averaging in standard models. In Grassl et al. [10], it was demonstrated that nonlocal models with standard rescaling tend to dissipate more energy close to boundaries than predicted by meso-scale analyses. The excessive energy dissipation was shown to be particularly pronounced for notched specimens. It was explained that including information from undamaged material below the notch in the averaging for points above the notch led to an increase in predicted strength and energy dissipation. Since this strengthening mechanism was particularly pronounced for notched specimens, it could make it difficult to predict the size effect of notched and

unnotched specimen with the same set of material parameters. In the same study, it was shown that nonlocal models with distance-based and stress-based averaging do not exhibit an excessive energy dissipation, if calibrated accordingly. Therefore, such models might be more suitable for predicting the size effect of notched and unnotched specimens with one set of parameters.

In [19], a standard rescaling model and a distance-based model, which is similar to the present distance based approach, were used to investigate numerically the size effects in notched and unnotched beams. In this study, the models were calibrated to fit theoretical size effect laws for notched and unnotched specimens simultaneously. It was found that with the distance based model a better fit was obtained than with the standard model. Furthermore, the input parameters needed for the best fits with the two models were very different. For instance, for the standard rescaling approach, a significantly greater fracture energy was required than for the distance based model. Already in this study, it was pointed out that experimental results would be required to conclude which of the two models provide physically more meaningful results. This will be the focus of the present study. However, motivated by the results in [10], a different approach has been chosen to assess the performance of the two nonlocal models. In [10], it was shown that the dissipated energy profiles for the distance-based and standard approaches are very similar for unnotched beams. Only for notched beams the standard approach significantly overestimates the dissipated energy close to boundaries. Therefore, we aim to determine the basic parameters of the two models only by fitting the results for the unnotched specimens. Thus, input parameters such as strength and fracture energy for the two models will only be determined from the unnotched beams of different size. With this approach, it is expected that the strength and fracture energy input of these models will be the same or at least very similar, which is different from [19]. For the standard model, no additional fitting will be carried out. Only for the distance-based model, we still need to determine the input parameters related to the reduction of the nonlocal length, since they cannot be obtained from the unnotched specimens alone.

The aim of the present study is to investigate the capability of integral-type nonlocal models to predict the size effect on strength for notched and unnotched concrete structures. In particular, the influence of the type of averaging near boundaries on the size effect for notched and unnotched specimens is investigated. The data of Hoover et al. [12] are used as the experimental basis. The performance of the standard and distance-based models is compared. The distance-based model is selected as a representative example of a model which can reduce the dissipation close to boundaries and is computationally efficient. Alternative approaches, such as crack band models and implicit gradient models, are briefly mentioned in the discussion.

## 2. Nonlocal models

Nonlocal formulations of a simple isotropic damage model are used for the size effect study in Section 3. These formulations have been previously presented in Grassl et al. [10] and Xenos et al. [25]. The stress  $\boldsymbol{\sigma}$  is linked to the strain  $\boldsymbol{\varepsilon}$  by the stress–strain law

$$\boldsymbol{\sigma} = (1 - \omega)\mathbf{D}_e : \boldsymbol{\varepsilon} = (1 - \omega)\tilde{\boldsymbol{\sigma}} \quad (1)$$

where  $\omega$  is the damage variable,  $\mathbf{D}_e$  is the isotropic elastic stiffness tensor based on Young's modulus  $E$  and Poisson's ratio  $\nu$ , and  $\tilde{\boldsymbol{\sigma}} = \mathbf{D}_e : \boldsymbol{\varepsilon}$  is the effective stress. The exponential softening curve shown in Fig. 1(a) is obtained if the damage variable  $\omega$  is considered as a function the history variable  $\kappa_d$  of the form

$$\omega(\kappa_d) = \begin{cases} 0 & \text{if } \kappa_d \leq \varepsilon_0 \\ 1 - \frac{\varepsilon_0}{\kappa_d} \exp\left(-\frac{\kappa_d - \varepsilon_0}{\varepsilon_f - \varepsilon_0}\right) & \text{if } \kappa_d \geq \varepsilon_0 \end{cases} \quad (2)$$

where  $\varepsilon_0$  and  $\varepsilon_f$  are two dimensionless parameters controlling the peak stress and the slope of the softening part of the stress–strain curve.

In the present model, the failure process is described exclusively by the nonlocal continuum approach. Even for very high damage values close to unity, it is assumed that no new traction-free surfaces are introduced.

The history variable  $\kappa_d$  is defined by

$$\kappa_d(t) = \max_{\tau \leq t} \bar{\varepsilon}_{\text{eq}}(\tau) \quad (3)$$

where the time variable  $t$  formally parameterises the history of the material and

$$\bar{\varepsilon}_{\text{eq}}(\mathbf{x}) = \int_V \alpha(\mathbf{x}, \boldsymbol{\xi}) \varepsilon_{\text{eq}}(\boldsymbol{\xi}) d\xi \quad (4)$$

is the nonlocal equivalent strain. At point  $\mathbf{x}$ , the nonlocal equivalent strain  $\bar{\varepsilon}_{\text{eq}}$  is evaluated as a weighted average of local equivalent strains  $\varepsilon_{\text{eq}}$  at points  $\boldsymbol{\xi}$  in the vicinity of  $\mathbf{x}$  within the integration domain  $V$ .

The local equivalent strain is evaluated as

$$\varepsilon_{\text{eq}} = \frac{1}{E} \sqrt{\sum_{l=1}^3 \tilde{\sigma}_l^2} \quad (5)$$

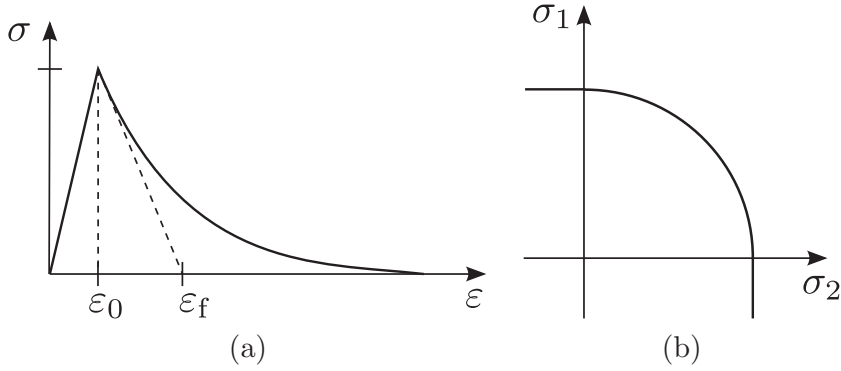


**Fig. 1.** Isotropic damage model: (a) stress–strain curve with softening, (b) modified Rankine strength envelope in the principal stress plane (assuming plane-stress conditions).

where  $\langle \dots \rangle$  is the positive-part operator and  $\tilde{\sigma}_I$ ,  $I = 1, 2, 3$ , are the principal values of the effective stress  $\tilde{\boldsymbol{\sigma}} \equiv \mathbf{D}_e : \boldsymbol{\varepsilon}$ . This definition of equivalent strain corresponds to the Rankine failure criterion with a smooth round-off in the region of multiaxial tension, as shown for the 2D (plane stress) case in Fig. 1(b).

The weight function in (4) is normalised to preserve uniform fields, i.e., it is defined as

$$\alpha(\mathbf{x}, \xi) = \frac{\alpha_0(\mathbf{x}, \xi)}{\int_V \alpha_0(\mathbf{x}, \zeta) d\zeta} \tag{6}$$

where  $\alpha_0(\mathbf{x}, \xi)$  is a function that would, in the standard averaging approach, depend exclusively on the distance between points  $\mathbf{x}$  and  $\xi$ , but in modified versions of nonlocal averaging can have a more general form. The modified approach considered here is the distance-based model described in [10]. The difference between the standard and distance-based averaging is schematically shown in Fig. 2, in which axes  $x$  and  $y$  are supposed to form the boundary of the body.

For the model with standard averaging in Fig. 2(a), the function  $\alpha_0$  is chosen as an exponential function

$$\alpha_0(\mathbf{x}, \xi) = \exp\left(-\frac{\|\mathbf{x} - \xi\|}{R}\right) \tag{7}$$

which contains a parameter  $R$  reflecting the internal material length.

For the distance-based averaging in Fig. 2(b), we set

$$\alpha_0(\mathbf{x}, \xi) = \exp\left(-\frac{\|\mathbf{x} - \xi\|}{\gamma(\mathbf{x})R}\right) \tag{8}$$

where the auxiliary dimensionless function  $\gamma(\mathbf{x})$  scales the internal length depending on the distance  $d(\mathbf{x})$  of point  $\mathbf{x}$  from the boundary. Initially, a piecewise linear function

$$\gamma(\mathbf{x}) = \begin{cases} \beta + (1 - \beta) \frac{d(\mathbf{x})}{\eta R} & \text{for } d(\mathbf{x}) < \eta R \\ 1 & \text{for } d(\mathbf{x}) \geq \eta R \end{cases} \tag{9}$$

was considered as the simplest choice. As shown in Grassl et al. [10], a more regular distribution of dissipated energy near a notch tip is obtained with an exponential function

$$\gamma(\mathbf{x}) = 1 - (1 - \beta) \exp\left(-\frac{d(\mathbf{x})}{\eta R}\right) \tag{10}$$

Here,  $\beta$  and  $\eta$  are two dimensionless model parameters that control the reduction of the internal length near boundaries. Right at the boundary, the internal length is reduced to  $\beta R$ . The size of the boundary layer affected by the reduction is  $\eta R$  for the linear function (9), while for the exponential function (10) the internal length tends to  $R$  only asymptotically, with a smooth transition between  $\gamma \approx \beta + (1 - \beta)d/\eta R$  for  $d \ll \eta R$  and  $\gamma \approx 1$  for  $d \gg \eta R$ .

The input parameters for the nonlocal model with standard averaging are Young’s modulus  $E$ , Poisson’s ratio  $\nu$ , dimensionless parameters  $\varepsilon_0$  and  $\varepsilon_f$ , and the internal length  $R$ . For the model with distance-based averaging, the additional dimensionless parameters are  $\beta$  and  $\eta$ . In the next section, these models are applied to the analysis of the experimental size effect study reported in Hoover et al. [12].

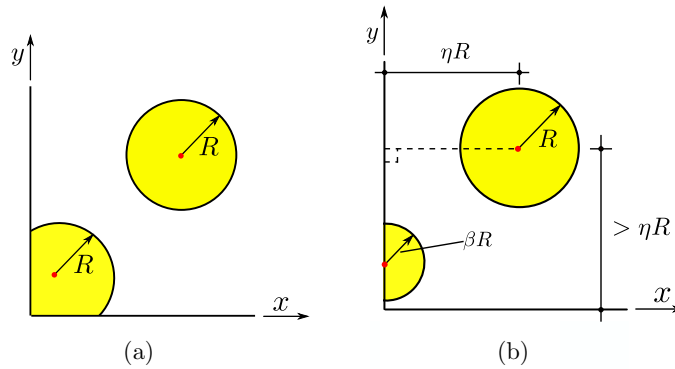


Fig. 2. Nonlocal averaging approaches near boundaries: (a) standard averaging and (b) distance-based averaging.

### 3. Size effect analysis

In this section, the tests of Hoover et al. [12] are analysed with the two nonlocal models presented in the previous section. The experimental program consisted of 128 concrete beams of four different sizes with varying notch depths, subjected to three-point bending. In the following section, the setup and geometry of the beams, and the calibration of the input parameters used for the analyses are described.

#### 3.1. Setup and input parameters

The geometry of the beams is shown in Fig. 3(a). All beam dimensions were scaled according to their depths except for the out-of-plane and notch thicknesses, which were kept constant at 40 mm and 1.8 mm, respectively. Four sizes of  $D = 500, 215, 94$  and 40 mm and four relative notch depths of  $\lambda = 0.3, 0.075, 0.025$  and 0 were used. The numerical analyses are based on a 2D plane-stress approximation using triangular constant-strain finite elements. One of the finite element meshes (with  $D = 40$  mm and  $\lambda = 0.3$ ) is shown in Fig. 3(b). The mesh in the central region of the beam is refined so that for all beam sizes and notch lengths the edge length of the triangular elements is approximately 1 mm. All numerical analyses of unnotched specimens are controlled indirectly by the crack mouth opening displacement, defined as the relative horizontal displacement of points A and B in Fig. 3(b). For the unnotched specimen ( $\lambda = 0$ ), the control points A and B are taken as two nodes close to each other at the bottom of the beam and at opposite sides of the vertical axis of symmetry. The experiments were also controlled by the relative horizontal displacement of two points, but the initial distance  $g$  between these points, called the gauge length, was not the same as in the simulations. In experiments, it varied for the different sizes and shapes according to Fig. 8 in [12].

To facilitate the comparison of results for specimens of different sizes, it is useful to transform the loading force  $F$  into the nominal stress,  $\sigma_N = 1.5FL/(bD^2)$ , which corresponds to the maximum stress obtained using the elastic beam theory for the unnotched beams. Here,  $L$  is the span,  $b$  the out-of-plane thickness and  $D$  the depth of the beam.

The two phenomenological nonlocal models presented in the previous section require several input parameters which cannot be taken directly from the experimental data provided in Hoover et al. [12]. Instead, an optimum set of parameters has to be determined by inverse analysis of the experiments. The fitting of the input parameters is performed in several steps. Firstly, the elastic parameters  $E$  and  $\nu$  are determined. Here, assuming that all concrete beams should have the same elastic properties, since they are made of the same batch of concrete, the biggest unnotched specimen ( $D = 500$  mm and  $\lambda = 0$ ) is used to determine Young's modulus,  $E = 35.6$  GPa, based on the initial slope of the load–displacement curve. The calibration is performed on the largest unnotched specimen, because the results for this specimen exhibit the least scatter and contain the greatest elastic range of all sizes and geometries. Poisson's ratio is taken directly from the experiments as  $\nu = 0.172$  [12].

Next, the parameters related to the inelastic response are determined by creating a database of the structural results for several configurations of input parameters. Firstly, this database is generated for parameters  $\varepsilon_0$ ,  $\varepsilon_f$  and  $R$  for the two models applied to the unnotched specimen. Parameters  $\beta$  and  $\eta$  of the distance-based model are not varied yet, because they are expected to have a very small influence on the response of the unnotched specimen, as demonstrated in Grassl et al. [10]. The considered ranges of input parameters used for these data are  $\varepsilon_0 = 0.12\text{--}0.15 \times 10^{-3}$ ,  $\varepsilon_f = 0.2\text{--}2 \times 10^{-3}$  and  $R = 1\text{--}8$  mm. The different configurations are generated by first selecting a nonlocal length  $R$  and then varying  $\varepsilon_0$  and  $\varepsilon_f$ . For each configuration, an error measure is computed based on the sum of the squares of differences between selected computational and experimental results. For the sizes  $D = 40\text{--}215$  mm, only the difference in peak loads is used for the error measure, since Young's modulus has been calibrated using the results for the largest specimen only. For  $D = 500$  mm, for which Young's modulus has been calibrated, the loads obtained in computations and experiments are compared at strain

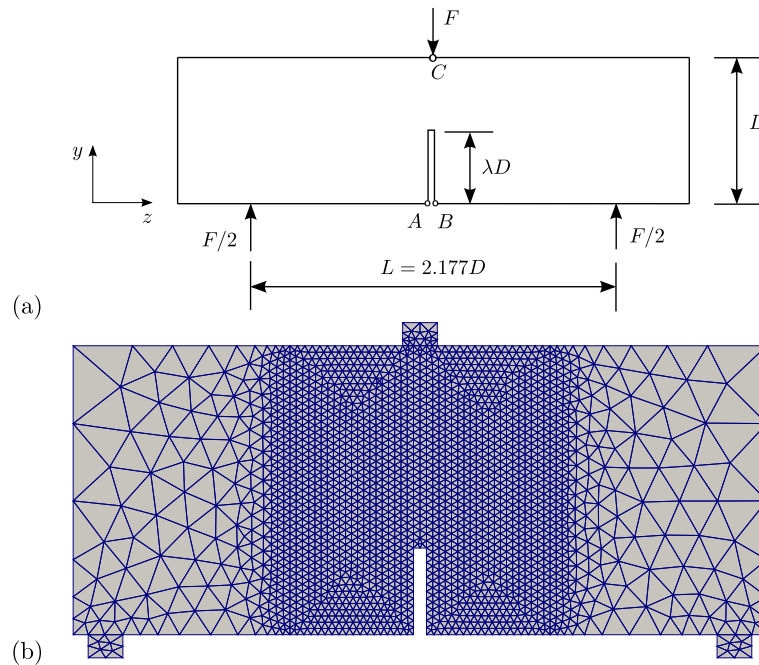


**Fig. 3.** Three-point bending beams used for size effect study: (a) geometry and loading setup and (b) finite element mesh.

levels equal to 0.8, 1, 1.25, 1.5, 2 and 3 times the strain at peak load. The differences for these six levels are multiplied by a weight of 1/6 to balance the importance of the measurements of each specimen. The minimum error is obtained for  $\varepsilon_0 = 0.14 \times 10^{-3}$ ,  $\varepsilon_f = 1.2 \times 10^{-3}$  and  $R = 2$  mm for both the standard and distance-based models. This shows that, for the selected nonlocal length  $R$  and for the unnotched specimens, the distance-based approach and the standard model yield very similar results. It should be noted that the difference in errors between the set with the smallest nonlocal length,  $R = 1$  mm, and the optimum one,  $R = 2$  mm, is negligible. The set with  $R = 2$  mm has been selected since it reduces the computational time required for the analyses. Although this value provides the best results for the range of nonlocal radii considered, it would be of interest for future studies to follow the approach in [25] and evaluate the fracture roughness in the experiments to see if the chosen nonlocal length matches the one which leads to the experimentally observed zone of dissipated energy. One of the potential drawbacks of inverse analyses based on global structural results, such as load–displacement curves and peak loads, is that the inverse fit might result in nonphysical local performances. Unfortunately, information on the roughness of the fracture surfaces obtained in the experiments has not been provided.

At this stage, the calibration of the standard model is complete. For the distance-based model, two additional parameters  $\beta$  and  $\eta$  need to be calibrated. This calibration is performed by fitting the peak load of the specimens with the longest notch ( $\lambda = 0.3$ ). Parameter  $\eta$  is set to its default value  $\eta = 1$  [10], whereas for the other parameter the range of  $\beta = 0.05$ – $0.5$  is considered. The minimum error is obtained for  $\beta = 0.05$ . This  $\beta$  is considerably smaller than  $\beta = 0.3$  obtained in [10] by fitting local dissipation profiles to meso-scale modelling results. Since for the experiments only structural data are available, it is not possible to make any direct judgement on the dissipation near the boundary. After the calibration, the determined input parameters are used in simulations of the entire set of results obtained experimentally in the size effect study of Hoover et al. [12].

### 3.2. Results

The results of simulations with the standard and distance-based models are compared with the experimental results of Hoover et al. [12] in the plot of nominal stress versus nominal strain in Fig. 4. For the experiments, results are shown as the mean (red<sup>1</sup> solid curve) and the range (red shaded area). The description of colours refers to the online version of the article.

In addition, the results are presented in Fig. 5 by plots of the nominal strength versus the specimen size (depth  $D$ ) for the two extreme values of the notch length ( $\lambda = 0$  and 0.3). The nominal strength,  $\sigma_{N,\max} = 1.5F_{\max}L/(bD^2)$ , is defined as the nominal stress at the peak load,  $F_{\max}$ .

The results in Figs. 4 and 5 show that the distance-based model can reproduce the experimental results well for all notch lengths and beam sizes. The standard nonlocal model (with parameters determined by fitting the experimental data for

<sup>1</sup> For interpretation of color in Fig. 4, the reader is referred to the web version of this article.

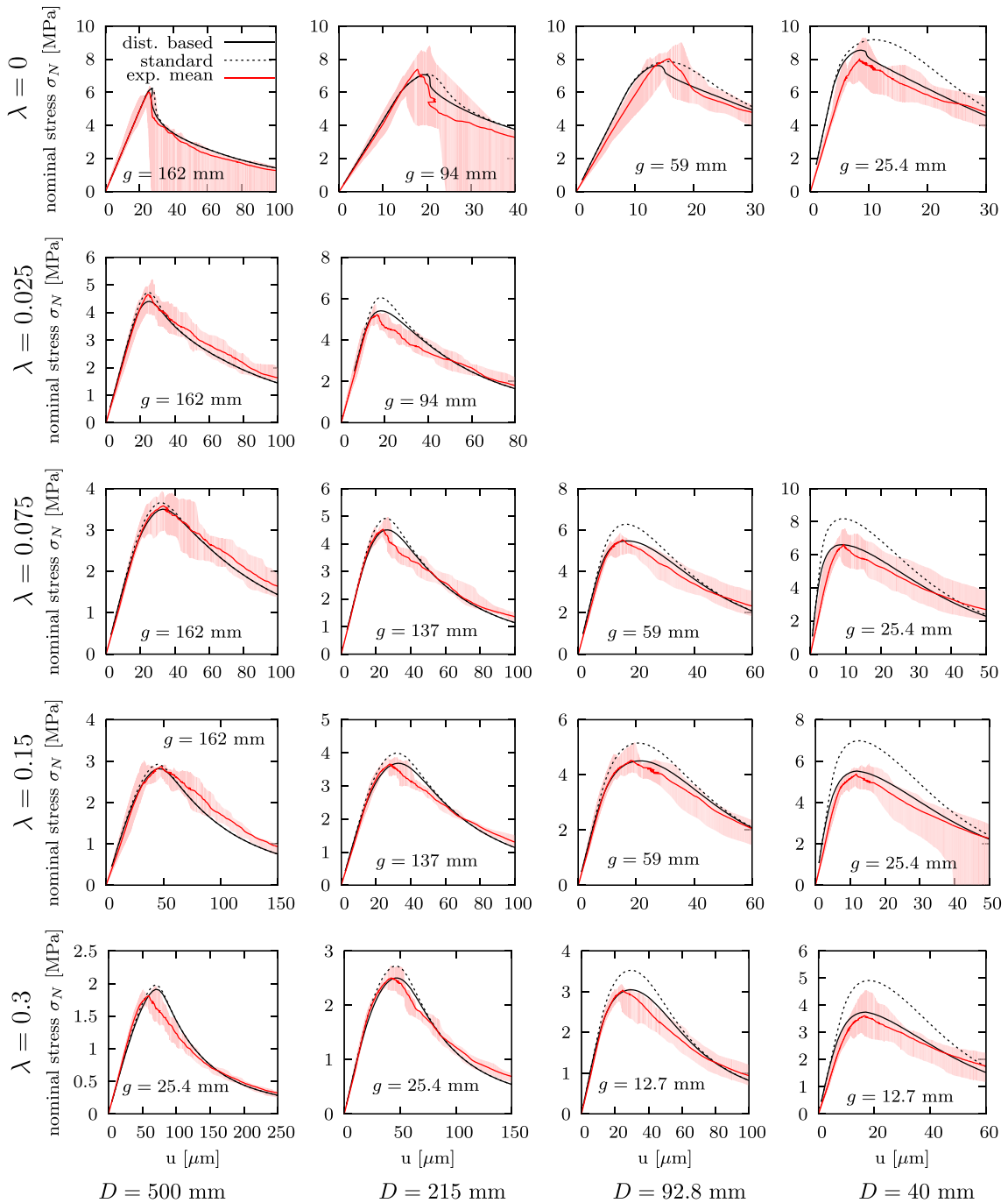


**Fig. 4.** Comparison of numerical results obtained with standard and distance-based nonlocal models with the experimental data reported in Hoover et al. [12]. The shaded region in the figures shows the range of the experimental results and  $g$  stands for gauge length.

unnotched beams) significantly overestimates the nominal strength of the small notched beams. For all large specimens, the fit obtained with the standard model is good (and is virtually the same as with the distance-based model). Consequently, for the experimental data available, the standard model fails to model size effect for different geometries (i.e., for specimens with different notch sizes). As shown in Figs. 4 and 5, this deficiency of the standard formulation can be eliminated by a modified nonlocal averaging near boundaries. The distance-based model, which reduces the nonlocal length near boundaries, can capture the experimental response for both notched and unnotched specimens. Of course, the

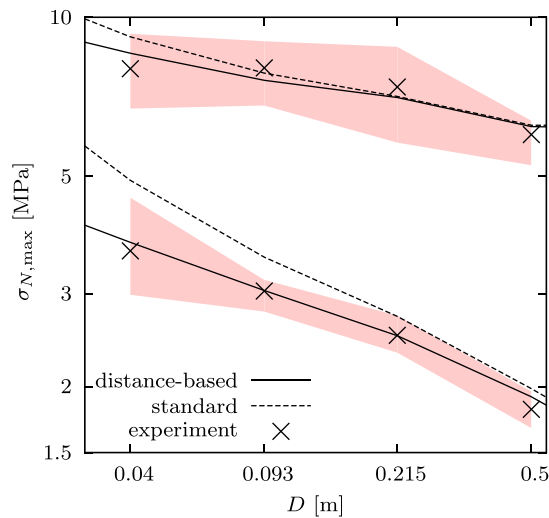


**Fig. 5.** Nominal strength versus beam depth for unnotched specimens ( $\lambda = 0$ ), specimens with biggest notch ( $\lambda = 0.3$ ) for the numerical simulations with standard and distance-based nonlocal approaches compared to experimental results. For the experimental results, the mean and the range of nominal strength (shaded region) is shown.

distance-based model requires additional parameters, which need to be calibrated using, for instance, experimental results of beams with different types of boundaries, as done here.

The reason why the standard model fails to reproduce the experiments is that it predicts too large dissipation near notches and, to a lesser extent, near unnotched boundaries [10]. This excessive energy dissipation becomes more pronounced if the nonlocal length is increased, since then more undamaged material is involved in the averaging process at points above the notch, which leads to lower nonlocal strain, lower damage and higher strength. To demonstrate this trend, additional analyses with a larger nonlocal length  $R$  are performed. For these analyses, all parameters are kept the same as before, except for  $R$  and parameter  $\varepsilon_f$ . For  $R = 4$  mm, parameter  $\varepsilon_f$  is adjusted to obtain a good fit with the 6 experimental points of the largest unnotched specimen used previously for the calibration of the parameters for the distance-based model. For  $R = 8$  mm, parameter  $\varepsilon_f$  is adjusted to obtain a good fit for the peak of the largest unnotched specimen only. The same parameters are then used for the standard model.

The influence of  $R$  on the overestimation of the strength of the notched specimens is shown in Fig. 6(a). The bigger the nonlocal length is, the stronger is the overestimation for the notched specimen with the standard model. The distance-based model is able to fit the results for both notched and unnotched specimens. In this demonstration of the influence of  $R$ , the calibration procedure has been simplified by changing  $R$  and  $\varepsilon_f$  only. Therefore, the standard model does not fit very well the peaks of the small sizes for the unnotched case (Fig. 6(b)). However, the mismatch is much smaller than for the notched case. If all parameters were readjusted, a somewhat better fit could be obtained, but the size effect for notched specimens would still be too strong. For the distance-based model, an increase of  $R$  leads to a slight reduction of the peak strength, which originates from a more significant reduction of the nonlocal length near boundaries.

#### 4. Discussion

In the previous section, the responses of the standard and distance-based nonlocal models were compared to the experiments reported in Hoover et al. [12]. It was shown that, within the available experimental range, the distance-based model provides good fits of data for notched as well as unnotched beams. On the other hand, the standard model with parameters calibrated on unnotched beams significantly overestimates the strength for notched beams of small sizes. Although the used experimental results are very comprehensive, the size range of the beams is still quite limited, since it is not practical to test very small or very large specimens. In contrast to experiments, numerical investigation of the limits is straightforward. Such a study can shed more light on the differences in the behaviour of individual models.

In particular, it is interesting to check how the distance-based model would behave for small sizes, since this model often uses a nonzero lower bound on the nonlocal length near boundaries. Therefore, there is a danger that the model might produce unexpected results for very small sizes. To explore this issue, the size effect on nominal strength for the two extreme cases of notched beams with  $\lambda = 0.3$  and unnotched beams with  $\lambda = 0$  is evaluated for a wider size range from  $1 \mu\text{m}$  to  $6 \text{m}$ . Of course, from the practical point of view, concrete specimens with dimensions smaller than the maximum aggregate size do not really represent the same material as sufficiently large specimens, and specimens with dimensions in the order of millimetres or microns cannot represent real concrete at all. But the scaling properties of a mathematical model can be studied without any limitations. The objective is not to describe what would happen for extremely small “concrete” specimens,

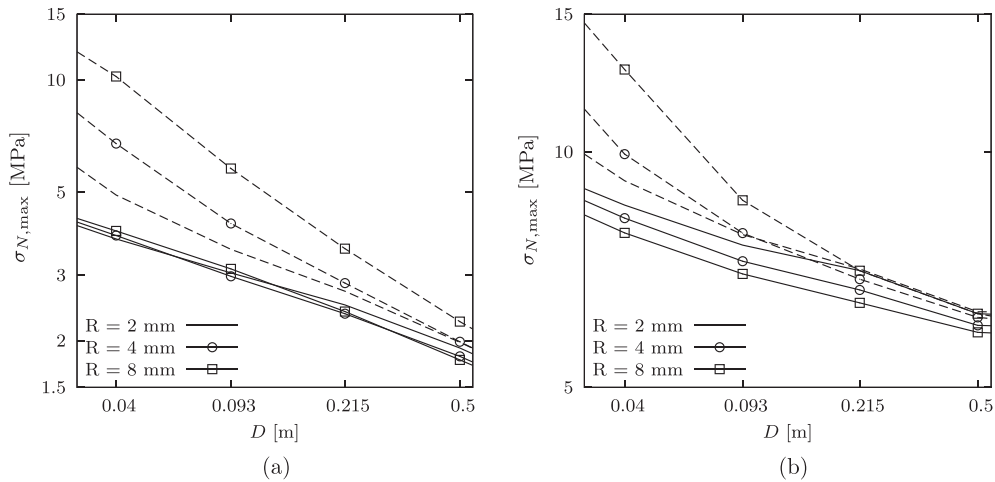


**Fig. 6.** Influence of nonlocal length on size effect prediction: nominal strength versus size for the standard (dashed lines) and distance-based model (solid lines) for (a) the notched and (b) the unnotched beam.

which cannot exist, but to better understand the asymptotic behaviour of the model, because asymptotic properties may partially affect the behaviour in the physically meaningful intermediate range.

Log-scale size effect diagrams for the nonlocal models used in the previous section for fitting of experimental results are shown in Fig. 7(a). Individual curves correspond to notched and unnotched specimens simulated using the standard and distance-based models. For notched specimens each diagram consists of two partially overlapping branches. The branch covering the range of sizes larger than or equal to the smallest tested specimen and plotted by a solid line was obtained with a fixed notch thickness, equal to 1.8 mm. This is the notch thickness used in the experiments for all tested sizes, which was also used in simulations leading to identification of optimal model parameters. In the extension of the numerical study to sizes above the experimental range, it was possible to keep the fixed notched thickness without any problems. However, in the extension to much smaller specimens, a fixed notch thickness would lead to a totally different geometry. The branch of the size effect curve covering the small-size range was thus obtained on finite element meshes with notch thicknesses scaled proportionally to other specimen dimensions, starting from the largest tested specimen. In Fig. 7(a), this branch is plotted by the dotted line. Within the experimental range, the difference between the results obtained with constant and scaled notch thicknesses remains small.

The large-size asymptote for notched specimens ( $\lambda = 0.3$ ) agrees well with the theory of linear elastic fracture mechanics, which gives nominal strength inversely proportional to the square root of size (in the log–log plot, the asymptote is a straight line of slope  $-1/2$ ; see the dashed line in Fig. 7(a)). For unnotched beams, the nominal strength is expected to approach the tensile strength of the material as the size tends to infinity. For parameters identified in the previous section, the uniaxial tensile strength is  $f_t = E\varepsilon_0 = 35.6 \text{ GPa} \times 0.14 \times 10^{-3} = 4.984 \text{ MPa}$ , which corresponds to the dotted horizontal line near the right border of Fig. 7(a). It might be somewhat surprising that the large-size asymptote is the dashed horizontal line at a slightly higher nominal strength level, namely at 5.499 MPa. To understand the origin of this apparent discrepancy, one should take into account that the theoretical limit is based on several simplifications, namely on standard assumptions of the beam theory and on the assumption that the specimen is loaded by a concentrated force. In reality, the cross sections do not remain perfectly planar, and the load is not applied at one single point. In the test, the loading force and the reactions at supports were transmitted to the concrete specimen by steel plates which distribute the concentrated forces, to avoid local crushing. The plates were glued to the specimen and interacted with it. In particular, the steel plate around midspan caused a deviation of the stress distribution in the middle cross section from the distribution corresponding to the simplified assumption that the bending moment is transmitted by the concrete part of the section only. Therefore, even in the elastic range, the maximum tensile stress does not exactly correspond to the theoretical value  $\sigma_N = 1.5FL/bD^2$ , which would be obtained according to beam theory applied to the concrete beam with no steel plates. The present finite element simulations take into account the presence of steel plates, and thus are closer to the experimental setup and provide a better approximation of the real phenomena than the simplified theory.

One could suppress the above mentioned effects by suitable adjustments of the finite element model, to obtain a numerical solution closer to the theoretical one. However, since the model parameters have been calibrated on experimental data, and since our finite element model is much closer to the real conditions than the simplified beam theory, we prefer to accept that the large-size asymptote does not correspond to  $\sigma_{N,\max} = f_t$ . Analysis of the numerically computed stress field shows that as long as the whole beam remains elastic, the maximum normal stress in concrete is  $\bar{\sigma}_N = 1.36FL/bD^2$ . If this were defined as the nominal stress, the corresponding nominal strength  $\bar{\sigma}_{N,\max}$  of extremely large specimens would indeed tend to  $f_t$ .

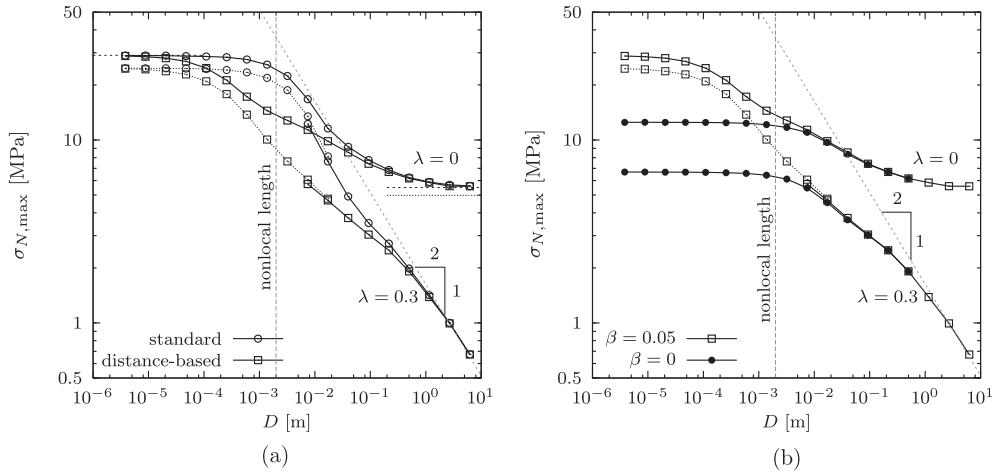


Fig. 7. Size effect plot (a) for the standard model and distance-based model with  $\beta = 0.05$ , and (b) for the distance-based model with  $\beta = 0.05$  and  $\beta = 0$ .

The small-size asymptotes in Fig. 7(a) are horizontal but, for both specimen geometries (notched and unnotched), at extremely large strength levels. High stresses arising in simulations of very small specimens can be attributed to the fact that if the specimen is much smaller than the nonlocal length, nonlocal averages are almost the same at all points of the specimen and are computed by averaging with an almost uniform weight. For the standard nonlocal model, this is the case if  $D \ll R$  where  $R$  is considered as a fixed constant. But even for the distance-based model with  $\beta > 0$ , the nonlocal averaging is performed with an almost uniform weight if  $D \ll \beta R$ . This explains why the horizontal small-size asymptotes in Fig. 7(a) for the standard model and for the distance-based model with  $\beta = 0.05$  coincide (of course if the shape of the specimen, given by the relative notch size  $\lambda$ , is fixed). With decreasing specimen size, the nominal strength obtained for the distance-based model with  $\beta = 0.05$  approaches the same limit as for the standard model, only “more slowly”, in the sense that the specimen must be about  $20\times$  smaller to get similar values of nominal strength.

For unnotched beams and nonzero parameter  $\beta$ , the ratio between the small-size and large-size asymptotic values of nominal strength can be evaluated from the elastic solution. For very large unnotched specimens, the peak load corresponds to the elastic limit state, at which the first material point attains the damage threshold. If the specimen dimensions are much larger than the internal length of the material, the nonlocal field is almost identical with the local field. Therefore, damage is initiated when the maximum local equivalent strain becomes equal to the elastic limit strain,  $\varepsilon_0$ . For extremely small unnotched specimens, the nonlocal model with  $\beta > 0$  gives an almost uniform nonlocal equivalent strain across the whole specimen, and so damage is initiated simultaneously at all points. It can be shown that this limit elastic state again corresponds to the peak load, but this time it is attained when the nonlocal equivalent strain becomes equal to  $\varepsilon_0$ . Consequently, the ratio between the small-size and large-size limits of nominal strength is equal to the ratio between the maximum local equivalent strain and the nonlocal equivalent strain (computed by averaging over the whole concrete beam with a uniform nonlocal weight function). For the specific unnotched beam geometry considered here, this ratio turns out to be 5.279, and the corresponding small-size asymptote is thus at nominal strength  $5.279 \times 5.499 \text{ MPa} = 29.03 \text{ MPa}$ ; see the dashed horizontal line near the left border of Fig. 7(a).

If the nonzero minimum value of nonlocal length is not enforced and parameter  $\beta$  is reduced to zero, the small-size nominal strength is substantially lower. It should be emphasised that if  $\beta$  is only reduced but still kept positive, the small-size asymptote remains the same as for larger  $\beta$  but is approached more slowly, which means that the nominal strength in the intermediate (i.e., realistic) size range is reduced. This analysis of the asymptotic behaviour shows that by setting a positive minimum nonlocal length in the distance-based model, one only shifts the problem of excessive strength of notched structures to smaller sizes. On the other hand, if  $\beta$  is set to zero, the asymptotic behaviour changes dramatically. The small-size asymptote is again a horizontal straight line, but the limit value of nominal strength is much smaller than for any positive  $\beta$ . This is documented in Fig. 7(b). For the unnotched specimens, the already mentioned small-size limit of nominal strength valid for the distance-based model with  $\beta > 0$  as well as for the standard model is 29.03 MPa but, for the distance-based model with  $\beta = 0$ , it was numerically found to be just 12.46 MPa. For the notched specimens with  $\lambda = 0.3$ , the small-size limit of nominal strength is 24.55 MPa for the distance-based model with  $\beta > 0$  as well as for the standard model, and just 6.68 MPa for the distance-based model with  $\beta = 0$ .

If  $\beta$  is set to zero, the dependence of characteristic length on the distance from the boundary is controlled by parameter  $\eta$ . For very small specimens, the characteristic length at each point  $\mathbf{x}$  is given by  $\eta d(\mathbf{x})$  where  $d$  denotes the distance from the boundary. This statement is exact for the model with linear function (9) and asymptotically valid for the model with exponential function (10), used in the present study. Consequently, in the small-size limit, the entire solution scales with the specimen size in the same way as in plasticity or other theories without a length parameter, because the internal length

at each point scales with the specimen size. This explains why the nominal strength tends to a constant. Its small-scale limit is independent of the “large-scale” characteristic length  $R$  and is controlled by parameter  $\eta$ . Therefore, the limit values of 12.49 MPa or 6.68 MPa mentioned in the previous paragraph correspond to the specific value of  $\eta = 1$  used in the present study, but could be adjusted by changing parameter  $\eta$ . The numerically evaluated dependence of the small-size limit of nominal strength,  $\sigma_{N,\max}^{(0)}$ , on parameter  $\eta$  is plotted in Fig. 8 for the specific set of parameters  $E$ ,  $\varepsilon_0$  and  $\varepsilon_f$  identified from experiments in the previous section. The results show that by changing  $\eta$  it is possible to obtain any desired value of small-size nominal strength between the large-size nominal strength and the small-size nominal strength for the standard model and distance-based model with  $\beta > 0$ .

Since the distance-based model with  $\beta = 0$  becomes local for points directly at the boundary, it can be expected that the dissipated energy per unit sectional area strongly depends on the specimen size. This dependence is shown in Fig. 9(a) for four very small beams with  $\lambda = 0.3$  and  $D = 3.2, 1.38, 0.59$  and  $0.11$  mm. In these diagrams, the nominal stress is plotted against the load–point displacement. The curves for specimens of different sizes differ in the pre-peak as well as in the post-peak ranges, which indeed indicates that the dissipated energy per unit area decreases with decreasing specimen size. Alternative approaches, such as cohesive crack and crack band models [4], which have been demonstrated to fit the present size effect results for different boundary geometries, are expected to produce a very different response, since they are by construction intended to reproduce a given energy dissipation per unit area, independently of the width of the fracture process zone. Therefore, it is expected that these models provide a dissipated energy per unit area which is independent of the specimen size. We have investigated this expected behaviour by applying a simple damage-based crack band model using the same equivalent strain definition as for the nonlocal model, but formulating the damage law as a function of the inelastic displacement and not of the strain [16]. The input for this model is the tensile strength and the fracture energy, which are calibrated as  $f_t = 5$  MPa and  $G_f = 60$  N m/m<sup>2</sup> to fit the response of the largest size specimen for  $\lambda = 0.3$ . In Fig. 9(b) it is shown that the crack band model provides a stress–displacement response which does not indicate a reduction of the dissipated energy with decreasing specimen size. On the contrary, in the range of relatively small displacements  $u$  shown in Fig. 9(b), the area below the curve moderately increases with decreasing specimen size.

Despite the very different size dependence of energy dissipated by the nonlocal distance-based model with  $\beta = 0$  and by the crack band model, the asymptotes of the two models for small sizes are both horizontal and at similar levels, as shown in Fig. 10. This confirms that for small sizes the material strength determines the structural strength.

It is not the purpose of the above comparison to support strong statements that distance-based nonlocal models perform better or worse than crack band approaches. From the literature, it is already known that crack band models can describe the present type of size effects satisfactorily [13]. Nonlocal models, on the other hand, have several key advantages over crack band models, such as being able to provide mesh-independent results for distributed cracking and crack directions which are less sensitive to the alignment of the finite element mesh [2].

Finally, let us add a few comments on the expected asymptotic behaviour of nonlocal damage models in the implicit gradient format [22,21]. Such models construct the nonlocal field as the solution of a boundary value problem (BVP), which typically consists of a second-order differential equation

$$\bar{\varepsilon}_{\text{eq}}(\mathbf{x}) - l^2 \nabla^2 \bar{\varepsilon}_{\text{eq}}(\mathbf{x}) = \varepsilon_{\text{eq}}(\mathbf{x}) \quad (11)$$

with a homogeneous Neumann boundary condition

$$\frac{\partial \bar{\varepsilon}_{\text{eq}}(\mathbf{x})}{\partial n} = 0 \quad (12)$$

in which  $l$  is the internal length parameter,  $\nabla^2$  is the Laplace operator, and  $\partial/\partial n$  denotes the derivative in the direction normal to the boundary. Formally, the solution of this BVP can be written in the integral form (4) with the nonlocal weight function  $\alpha(\mathbf{x}, \xi)$  defined as the Green function of the BVP [22]. For a one-dimensional problem solved on an infinite domain (the whole real axis), the Green function would be a scalar multiple of the exponential function (7), with  $R = l$ , and the implicit gradient formulation would be equivalent to the present nonlocal integral formulation. In multiple dimensions, analytical expressions for the Green function are available for infinite domains only, and even then they differ from (7). One important difference is that the Green function is always symmetric with respect to arguments  $\mathbf{x}$  and  $\xi$ , which is not the case for the nonlocal weight function constructed by standard scaling (6), nor for the distance-based nonlocal weight function (8). Therefore, the implicit gradient formulation reflects the proximity of boundaries in a somewhat different way.

A detailed numerical study of the size effect obtained with the implicit gradient formulation is out of scope of the present paper. Nevertheless, the unpublished results on dissipation density near notches presented by the third author at a conference [17] indicate that the excessive dissipation obtained with the implicit gradient model is similar to that obtained with the standard nonlocal integral model (if the shielding effect of the notch is accounted for). It can thus be expected that the problems with fitting of size effect data will be similar for both models. This can be further confirmed by the following theoretical analysis of asymptotic properties in the small-size limit.

Consider a structure or specimen of a fixed shape but with a variable characteristic size  $D$ . By transformation of the spatial variables  $\mathbf{x}$  to the dimensionless variables  $\xi = \mathbf{x}/D$ , we can map the structure to a domain  $\Omega$  that does not depend on size  $D$ . Since  $\partial/\partial \mathbf{x} = (1/D)\partial/\partial \xi$ , Eq. (11) can be transformed into

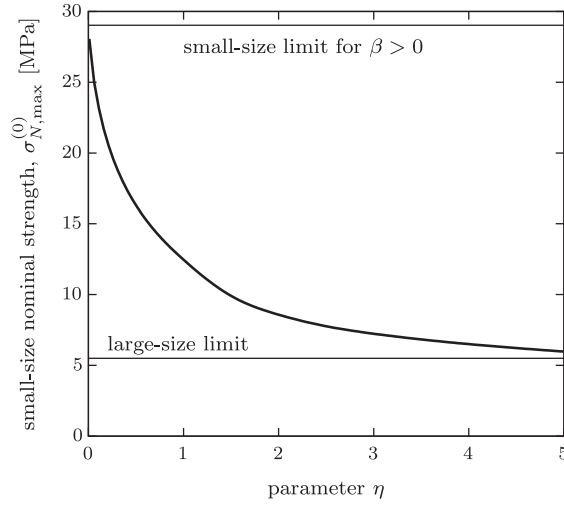


**Fig. 8.** Dependence of the small-size limit of nominal strength,  $\sigma_{N,max}^{(0)}$ , on parameter  $\eta$  (for the unnotched specimens and distance-based nonlocal model with  $\beta = 0$ ).

$$D^2 (\bar{\varepsilon}_{eq}(\xi) - \varepsilon_{eq}(\xi)) = l^2 \nabla_{\xi}^2 \bar{\varepsilon}_{eq}(\xi) \tag{13}$$

and, in the limit for  $D \rightarrow 0$ , it reduces to the Laplace equation

$$\nabla_{\xi}^2 \bar{\varepsilon}_{eq}(\xi) = 0 \tag{14}$$

The subscript “ $\xi$ ” at  $\nabla^2$  emphasises that the derivatives are taken with respect to the dimensionless coordinates  $\xi$ . The solution of Eq. (14) with boundary condition (12) is  $\bar{\varepsilon}_{eq}(\xi) = c$  where  $c$  is an arbitrary constant. Non-uniqueness of the solution is a consequence of complete neglect of the terms with  $D$  in Eq. (13). For very small but finite  $D$ , the solution is close to a constant, but this constant is not arbitrary. To determine its value, we integrate Eq. (13) over the domain  $\Omega$ , transform the integral of  $\nabla_{\xi}^2 \bar{\varepsilon}_{eq}$  to a surface integral using the divergence theorem, and apply boundary condition (12):

$$D^2 \int_{\Omega} (\bar{\varepsilon}_{eq}(\xi) - \varepsilon_{eq}(\xi)) d\Omega = l^2 \int_{\Omega} \nabla_{\xi}^2 \bar{\varepsilon}_{eq}(\xi) d\Omega = l^2 \int_{\partial\Omega} \frac{\partial \bar{\varepsilon}_{eq}(\xi)}{\partial n} d\partial\Omega = 0 \tag{15}$$

This implies that, for any  $D > 0$ ,

$$\int_{\Omega} \bar{\varepsilon}_{eq}(\xi) d\Omega = \int_{\Omega} \varepsilon_{eq}(\xi) d\Omega \tag{16}$$

and thus the limit solution, approached asymptotically for  $D \rightarrow 0$ , is

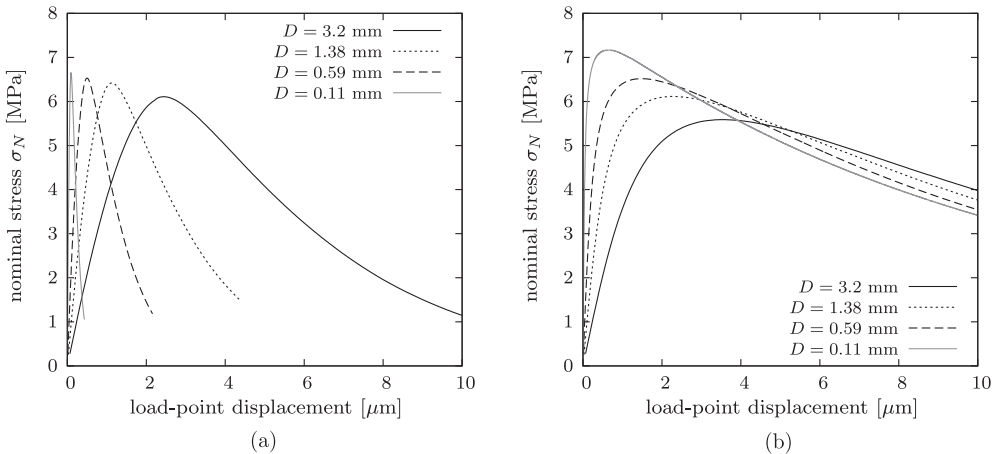


**Fig. 9.** Nominal stress–displacement curves for four very small notched specimens for (a) distance-based nonlocal model with  $\beta = 0$  and (b) crack band model.

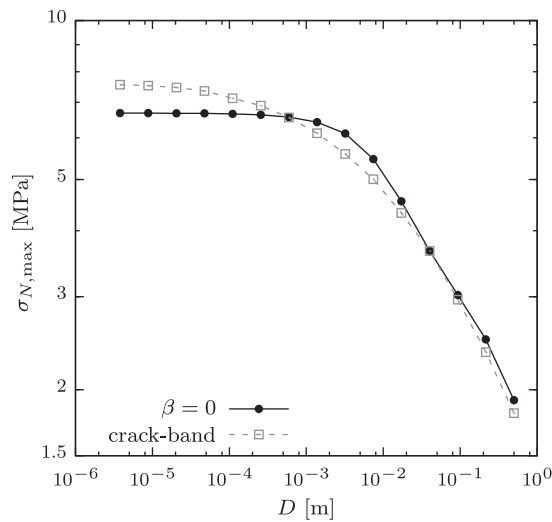


**Fig. 10.** Nominal strength versus size for the distance-based model with  $\beta = 0$  and for the crack band model, computed for notched specimens with  $\lambda = 0.3$ .

$$\bar{\varepsilon}_{\text{eq}}(\xi) = \frac{1}{|\Omega|} \int_{\Omega} \varepsilon_{\text{eq}}(\xi) d\Omega \quad (17)$$

where  $|\Omega|$  is the measure (area in 2D and volume in 3D) of the reference domain  $\Omega$ . Consequently, for very small specimens (compared to the characteristic length  $l$ ), the nonlocal field obtained from the BVP is close to the uniform field obtained by averaging of the local field with a uniform weight, and the small-size asymptotic behaviour of the implicit gradient model is the same as the asymptotic behaviour of the standard nonlocal integral model.

## 5. Conclusions

The present study on the prediction of size effect on strength of notched and unnotched beams made of quasibrittle materials with two nonlocal models with different ways of treating boundaries resulted in the following conclusions. Both the standard rescaling and the distance-based integral-type nonlocal damage models can predict the experimental size effect results well for one type of boundary with one set of input parameters. However, only the distance-based model is capable to provide a good agreement for both unnotched and notched beams with the same set of parameters. The small-size asymptotes of both models correspond to unrealistically high strength values. For the distance-based model, this deficiency is significantly alleviated by setting the lower limit of the internal length to zero.

## Acknowledgements

P. Havlásek has been financially supported by the European Social Fund under the project on Support of Inter-Sectoral Mobility and Quality Enhancement of Research Teams at the Czech Technical University in Prague (CZ.1.07/2.3.00/30.0034). P. Grassl acknowledges funding received from the UK Engineering and Physical Sciences Research Council (EPSRC) under grant EP/I036427/1 and funding from Radioactive Waste Management Limited (RWM) (<http://www.nda.gov.uk/rwm>), a wholly-owned subsidiary of the Nuclear Decommissioning Authority. RWM is committed to the open publication of such work in peer reviewed literature, and welcomes e-feedback to [rwmfeedback@nda.gov.uk](mailto:rwmfeedback@nda.gov.uk). M. Jirásek has been financially supported by the Czech Science Foundation (GAČR) under project 13-18652S. The numerical analyses have been performed with OOFEM, an open-source object-oriented finite element program [20] extended by the present authors. The finite element meshes have been prepared with the T3D mesh generator [24].

## References

- [1] Bažant ZP. Nonlocal damage theory based on micromechanics of crack interactions. *J Engng Mech, ASCE* 1994;120:593–617.
- [2] Bažant ZP, Jirásek M. Nonlocal integral formulations of plasticity and damage: survey of progress. *J Engng Mech, ASCE* 2002;128:1119–49.
- [3] Bažant ZP, Le JL, Hoover CG. Nonlocal boundary layer (NBL) model: overcoming boundary condition problems in strength statistics and fracture analysis of quasibrittle materials. In: *Fracture mechanics of concrete and concrete structures*, Jeju, Korea; 2010. p. 135–43.
- [4] Bažant ZP, Oh BH. Crack band theory for fracture of concrete. *Mater Struct* 1983;16:155–77.
- [5] Bellégo CL, Dubé JF, Pijaudier-Cabot G, Gérard B. Calibration of nonlocal damage model from size effect tests. *Eur J Mech A/Solids* 2003;22:33–46.
- [6] Bolander J, Hikosaka H. Simulation of fracture in cement-based composites. *Cem Concr Compos* 1995;17:135–45.
- [7] Eliáš J, Vořechovský M, Skoček J, Bažant Z. Stochastic discrete meso-scale simulations of concrete fracture: comparison to experimental data. *Engng Fract Mech* 2015;135:1–16.

- [8] Giry C, Dufour F, Mazars J. Stress-based nonlocal damage model. *Int J Solids Struct* 2011;48:3431–43.
- [9] Grassl P, Grégoire D, Solano LR, Pijaudier-Cabot G. Meso-scale modelling of the size effect on the fracture process zone of concrete. *Int J Solids Struct* 2012;49:1818–27.
- [10] Grassl P, Xenos D, Jirásek M, Horák M. Evaluation of nonlocal approaches for modelling fracture near nonconvex boundaries. *Int J Solids Struct* 2014;51:3239–51.
- [11] Grégoire D, Rojas-Solano LB, Pijaudier-Cabot G. Failure and size effect for notched and unnotched concrete beams. *Int J Numer Anal Methods Geomech* 2013;37:1434–52.
- [12] Hoover C, Bažant ZP, Vorel J, Wendner R, Hubler M. Comprehensive concrete fracture tests: description and results. *Engng Fract Mech* 2013;114:92–103.
- [13] Hoover CG, Bažant ZP. Cohesive crack, size effect, crack band and work-of-fracture models compared to comprehensive concrete fracture tests. *Int J Fract* 2014;187:133–43.
- [14] Jirásek M, Bažant ZP. Localization analysis of nonlocal model based on crack interactions. *J Engng Mech, ASCE* 1994;120:1521–42.
- [15] Jirásek M, Bažant ZP. *Inelastic analysis of structures*. Chichester: John Wiley and Sons; 2002.
- [16] Jirásek M, Grassl P. Evaluation of directional mesh bias in concrete fracture simulations using continuum damage models. *Engng Fract Mech* 2008;75:1921–43.
- [17] Jirásek M, Horák M. Regularized damage-plastic models: integral vs. gradient formulations. In: Oliver J, Jirásek M, Allix O, Moës N, editors. *Computational modeling of fracture and failure of materials and structures*. Barcelona: CIMNE; 2011. p. 300.
- [18] Jirásek M, Rolshoven S, Grassl P. Size effect on fracture energy induced by non-locality. *Int J Numer Anal Methods Geomech* 2004;28:653–70.
- [19] Krayani A, Pijaudier-Cabot G, Dufour F. Boundary effect on weight function in nonlocal damage model. *Engng Fract Mech* 2009;22:17–31.
- [20] Patzák B. OOFEM – an object-oriented simulation tool for advanced modeling of materials and structures. *Acta Polytech* 2012;52:59–66.
- [21] Peerlings RHJ, de Borst R, Brekelmans WAM, Geers MGD. Gradient enhanced damage modelling of concrete fracture. *Mech Cohes-Frict Mater* 1998;3:323–42.
- [22] Peerlings RHJ, de Borst R, Brekelmans WAM, de Vree JHP. Gradient-enhanced damage for quasi-brittle materials. *Int J Numer Methods Engng* 1996;39:3391–403.
- [23] Pijaudier-Cabot G, Bažant ZP. Nonlocal damage theory. *J Engng Mech, ASCE* 1987;113:1512–33.
- [24] Rypí D. *Sequential and parallel generation of unstructured 3D meshes*. PhD thesis. Czech Technical University. Prague, Czech Republic; 1998.
- [25] Xenos D, Grégoire D, Morel S, Grassl P. Calibration of nonlocal models for tensile fracture in quasi-brittle heterogeneous materials. *J Mech Phys Solids* 2015;82:48–60.